Global modelling of tropospheric iodine aerosol

Tomás M. Sherwen[1], Mat J. Evans[1,2], Dominick V. Spracklen[3], Lucy J. Carpenter[1], Rosie Chance[1], Alex R. Baker[4], Johan A. Schmidt[5], and Thomas J. Breider[6]

Key points:

- Model of iodine aerosol shows skill in reproducing observations
- Highest iodine mass is in the tropical marine-boundary layer, up to 101 % of DMS sulfate aerosol
- Regionally iodine aerosol is up to 11% of total sulfate, and higher (∼21 %) in the pre-industrial

Corresponding author: Tomás M. Sherwen, Wolfson Atmospheric Chemistry Laboratories, Department of Chemistry, University of York, York, YO10 5DD, UK (tomas.sherwen@york.ac.uk)

[1]Wolfson Atmospheric Chemistry Laboratories, Department of Chemistry, University of York, York, YO10 5DD, UK

[2]National Centre for Atmospheric Science, University of York, York, YO10 5DD

This article has been accepted for publication and undergone full peer review but has not been through the copyediting, typesetting, pagination and proofreading process, which may lead to differences between this version and the Version of Record. Please cite this article as doi: 10.1002/2016GL070062

Natural aerosols play a central role in the Earth system. The conversion of dimethyl sulfide to sulfuric acid is the dominant source of oceanic secondary aerosol. Ocean emitted iodine can also produce aerosol. Using a GEOS-Chem model we present a simulation of iodine aerosol. The simulation compares well with the limited observational dataset. Iodine aerosol concentrations are highest in the tropical marine-boundary layer (MBL) averaging 5.2 ng (I) m^{-3} with monthly maximum concentrations of 90 ng (I) m^{-3}. These masses

[3]Institute for Climate and Atmospheric and Science, School of Earth and Environment, University of Leeds, Leeds, LS2 9JT

[4]Centre for Ocean and Atmospheric Sciences, School of Environmental Sciences, University of East Anglia, Norwich, NR4 7TJ, UK

[5]Department of Chemistry, University of Copenhagen, Copenhagen, DK-2100, Denmark

[6]John A. Paulson School of Engineering and Applied Sciences, Harvard University, Cambridge, Massachusetts, USA

are small compared to sulfate (0.75% of MBL burden, up to 11% regionally) but are more significant compared to DMS sourced sulfate (3% of the MBL burden, up to 101% regionally). In the pre-industrial, iodine aerosol makes up 0.88 % of the MBL burden sulfate mass and regionally up to 21%. Iodine aerosol may be an important regional mechanism for ocean-atmosphere interaction.

1. Introduction

Atmospheric aerosols are important for climate as they scatter solar radiation and change cloud properties [*Stocker et al.*, 2000], with secondary aerosols playing a significant role [*Stocker et al.*, 2000]. Anthropogenic activities have changed their global distribution and abundance, but to understand the impact of these aerosols both natural and anthropogenic sources need to be well understood [*Carslaw et al.*, 2013]. The oceans cover most of the planet and for the last four decades the most important oceanic secondary source of aerosols has been thought to be the emission of dimethyl sulfide (DMS) and its oxidation to H_2SO_4 [*Lovelock et al.*, 1972; *Fitzgerald*, 1991]. Recent evidence for significant emissions of iodine from the ocean [*Carpenter et al.*, 2013; *MacDonald et al.*, 2014], coupled to previous coastal studies of iodine aerosol production [*O'Dowd et al.*, 2002], suggests the potential for an additional ocean aerosol source from iodine.

The presence of iodine in both the gas and aerosol phase in the marine-boundary layer (MBL) has been established over the last few decades [*Saiz-Lopez et al.*, 2012a]. Oceanic emissions of methyl iodide was considered the dominant source for many years, but studies have shown that emission of other iodinated hydrocarbons from the open and coastal ocean play an important role [*Jones et al.*, 2010; *Saiz-Lopez et al.*, 2012a]. More recently, inorganic iodine compounds (I_2, HOI) produced in the ocean surface layer from the reaction of O_3 with iodide are thought to be the dominant global source of iodine [*Carpenter et al.*, 2013]. Observations, box modeling and global model studies [*Saiz-Lopez and von Glasow*, 2012; *Saiz-Lopez et al.*, 2014; *Sherwen et al.*, 2016a, b] in coastal and remote sites have shown the ability of iodine to impact the concentration of O_3 and oxidants. Similar

studies in coastal and polar sites have shown that gas-phase iodine compounds can form low volatile gas-phase products which can both condense onto pre-existing aerosol and nucleate to form new particles [*O'Dowd et al.*, 2002; *Allan et al.*, 2015; *Roscoe et al.*, 2015; *Sellegri et al.*, 2016]. Open-ocean observations are sparse but suggest iodine aerosol concentrations in the range of 0.1-17 ng (I) m^{-3} [*Baker*, 2004, 2005; *Gilfedder et al.*, 2010; *Lai et al.*, 2008; *Rancher and Kritz*, 1980]. Aerosol iodine is composed of both inorganic and organic forms [*Baker*, 2005] with a complex aerosol phase chemistry [*Pechtl et al.*, 2007]. It is believed that iodine higher oxides (I_xO_y), formed through the self-reaction of iodine oxides (IO and OIO), and hydroiodic acid (HI) are the gas-phase condensables predominantly responsible for production of the iodine aerosol [*Saiz-Lopez et al.*, 2012a].

Recent advances in the representation of iodine in global chemical-transport models [*Saiz-Lopez et al.*, 2012b, 2014; *Sherwen et al.*, 2016a, b] allows us, for the first time, to simulate the global distribution of iodine aerosol. Here we describe simulations of tropospheric iodine aerosol within the GEOS-Chem chemical transport model, compare the calculated iodine masses against observations and evaluate its impact as a source of secondary aerosol for the present-day and pre-industrial.

2. Model setup

This work uses GEOS-Chem (www.geos-chem.org) version v10 at 4^ox5^o resolution with a coupled halogen chemistry scheme as described and evaluated for present-day [*Sherwen et al.*, 2016b] and for the pre-industrial [*Sherwen et al.*, 2016c]. This incorporates previous halogen development in GEOS-Chem [*Bell et al.*, 2002; *Eastham et al.*, 2014; *Parrella et al.*, 2012; *Schmidt et al.*, 2016; *Sherwen et al.*, 2016a], with gas-phase chemistry based

on JPL/IUPAC recommendations [*Sander et al.*, 2011; *Atkinson et al.*, 2006, 2007, 2008] and heterogeneous chemistry from previous work [*Abbatt et al.*, 2012; *Braban et al.*, 2007; *Ammann et al.*, 2013; *Sherwen et al.*, 2016a]. Short-lived iodo-carbons (CH_3I, CH_2I_2, CH_2ICl, CH_2IBr) are emitted using the inventory of *Ordóñez et al.* [2012]. HOI and I_2 are emitted from the ocean surface, using the parameterisation of *Carpenter et al.* [2013] which is uses surface O_3 concentration and oceanic iodide concentration [*MacDonald et al.*, 2014]. We run the model for two years (2004 and 2005) ignoring the first year as "spin-up" and using the final year for analysis.

We consider three iodine aerosol tracers based on the uptake of gas-phase iodine species onto coarse and accumulation mode sea-salt aerosol and onto sulfate aerosol. The uptake of iodine species (HI, HOI, INO_2, INO_3, I_2O_2, I_2O_3, I_2O_4) to these aerosols can lead to the iodine being permanently deposited onto that aerosol depending upon species, the aerosol type and its pH (see SI Table S1 and *Sherwen et al.* [2016b] for details). The physical properties of the iodine aerosol tracers are assumed to be the same as its parent aerosol as previously described [*Alexander et al.*, 2012; *Jaeglé et al.*, 2011]. We do not consider uptake of iodine species onto aerosol types where these processes lack experimental constraint (e.g. black carbon and dust, *Sherwen et al.* 2016a, b), and this probably causes an underestimate in the iodine aerosol in some regions which are subject to dust or biomass burning emissions. Significant uncertainty exists as to the chemical speciation of the iodine in aerosol, with iodide, iodate and organic iodine compounds all being present [*Baker*, 2005]. The speciation of iodine in aerosol is not considered here, only total aerosol iodine concentrations (in units of ng (I) m^{-3}).

Oceanic non-iodine secondary aerosol processes in the model are described elsewhere [*Park et al.*, 2004; *Alexander*, 2005]. In the GEOS-Chem version used here (v10), DMS emissions are calculated from an ocean-water climatology [*Kettle et al.*, 1999] and a transfer velocity [*Liss and Merlivat*, 1986]. They amount to 16.6 Tg (S) yr^{-1} (21 % of the global sulfur emission of 78.8 Tg (S) yr^{-1} in the model). This is ∼6 times the oceanic iodine emission of 2.75 Tg (I) yr^{-1} [*Sherwen et al.*, 2016b]. Iodine and DMS emissions are essentially uncorrelated due to their differing sources (see SI Fig. S1). Relative spatial contributions are considered further in Section 3. DMS contribution to total aerosol sulfate is estimated through a perturbation experiment. Assuming a linear model response, this allows the fraction of the sulfate that is due to DMS within the simulation to be determined. Globally, a 10 % increase in DMS emissions leads to a 2.17 % increase in sulfate deposition to 15.2 Tg (S) yr^{-1}. From this we conclude that 21.7 % of the global burden of sulfate comes from DMS, consistent with previous work [*Rap et al.*, 2013], and a DMS to sulfate conversion efficiency of 19.5 %.

To probe the possible changes of iodine aerosol between pre-industrial and the present-day, the model was also run with pre-industrial emissions as described previously [*Parrella et al.*, 2012; *Sherwen et al.*, 2016c]. Anthropogenic emissions of O_3 precursors are switched off and natural emissions maintained at their present-day values. Biomass-burning emissions are scaled to 10 % of the present-day. Natural sources of sulfur from DMS and volcanos are unchanged but anthropogenic sourced are switch off. Emissions of iodinated hydrocarbons are unchanged (they are presumed entirely natural). Ocean iodide concen-

trations are unchanged but the O_3 dependence of the emissions parameterisation allows inorganic iodine emissions to change.

3. Results

3.1. Present-day iodine aerosol

We calculate a global iodine emission of 2.75 Tg (I) yr^{-1} (2.2 Tg (I) yr^{-1} from inorganic species (I_2, HOI) and 0.6 Tg (I) yr^{-1} from organic species) as described in [*Sherwen et al.*, 2016b] and consistent with previous studies [*Saiz-Lopez et al.*, 2014; *Sherwen et al.*, 2016a]. Although iodine emissions are, on a per area basis, highest in coastal waters, the tropical open-ocean is so large it dominates the total global emission (SI Fig. S1). These emissions rapidly photolyse, leading to a complex gas-phase chemistry [*Saiz-Lopez et al.*, 2012a], deposition or the production of iodine aerosol.

The model's ability to simulate surface and vertical iodine oxide (IO) concentrations has previously been assessed against observations by *Sherwen et al.* [2016b]. The self reactions of IO and OIO lead to the production of iodine higher oxides [*Saiz-Lopez et al.*, 2012a], which together with uptake of HI (see Section 2) and other iodine compounds cause increases in iodine aerosol mass [*O'Dowd et al.*, 2002]. The surface concentrations of key gas-phase iodine species are shown in SI Fig. S2, with iodine aerosol mass concentrations at the surface calculated in the range 0.01 to 90 ng (I) m^{-3} in the monthly means with annual-means of 0.01-31 ng (I) m^{-3} (Fig. 1). The global modelled surface iodine aerosol concentrations are plotted on a monthly basis in the supplementary information (SI Figure S6).

Iodine aerosol is primarily located in the tropics, where the emission sources are largest (see Figures 1 and 3 in *Sherwen et al.* 2016b), with tropical marine-boundary-layer concentrations of at least 2.6 ng (I) m^{-3} in the annual mean. Highest concentrations are found within the Arabian Sea, the Bay of Bengal and off the Atlantic coast of central Africa. Concentrations fall off rapidly with altitude (SI Fig. S3). Modelled iodine aerosol concentrations in polar regions are small (SI Figures S3 and S4), compared to observations [*Alicke et al.*, 1999; *McElroy et al.*, 1999; *Hausmann and Platt*, 1994; *Saiz-Lopez et al.*, 2007; *Tuckermann et al.*, 1997]. This probably highlights the missing snow/ice related processes in the model. We find a global annual-mean iodine aerosol burden of 2.5 Gg (I), with 2.0 Gg (I) in the marine-boundary layer, and a globally averaged conversion efficiency of iodine emission into aerosol of 15.3 %. We calculate this as the ratio between the global emission of iodine (Tg (I) yr^{-1}) and the global deposition of aerosol tracers (Tg (I) yr^{-1}). This efficiency is uncertain and it is controlled by the chemistry scheme and notably by the fate of higher oxide chemistry for which our understanding is poor [*Sommariva et al.*, 2012; *Simpson et al.*, 2015; *Sherwen et al.*, 2016a].

3.2. Observational comparisons

Iodine aerosol observations are sparse, however comparisons to the available observations of non-polar open-ocean iodine aerosol are shown in Fig. 1 and in the supplementary information (Table S1). The model-calculated iodine aerosol mass concentrations are extracted from the model for the month and region of the observation (Fig. 1(top)). Due to the scarcity of marine aerosol iodine observations, data for total soluble iodine from cruises "M55" and "AMT13" [*Baker*, 2005] is included alongside other total iodine concentrations

in the comparison (see Table S1). Unpublished iodine aerosol data from cruises "D325" , "D357', and "D361' are also included (Table S1), with a description of their processing as discussed previsously [*Baker et al.*, 2001; *Chance et al.*, 2015; *Powell et al.*, 2015] and raw data (Table S3) given in the SI.

Although there is a degree of scatter, the model appears broadly consistent with the observations with some indication of a model over-estimate. The observations are not in the regions where the model predicts its highest concentrations and further observations in these regions would be very useful. We therefore conclude that given the current observational dataset, and the significant uncertainties in the modelled chemistry and aerosol processes [*Sherwen et al.*, 2016a; *Sommariva et al.*, 2012] the model provides a useful simulation of iodine aerosol.

3.3. Comparisons with other secondary aerosol sources

In order to place the calculated iodine aerosol mass into a wider secondary-aerosol context we compare it to the calculated sulfate aerosol. For consistency we consider sulfate aerosol in the same elemental terms as we use for iodine aerosol (ng (S) m^{-3}). Figure 2 shows the annual-mean surface concentrations of the sulfate (total and from DMS) and their mass (I/S) ratio (as a %) compared to the iodine aerosol (zonal comparison in SI Fig. S5). The highest total sulfate aerosol is found over SE Asia, Europe and North America where the anthropogenic source is highest. These concentrations rapidly decay away from the sources. Over the ocean, total sulfate concentrations become much smaller (29-452 ng (S) m^{-3} 5^{th} to 95^{th} percentiles of annual mean). Highest DMS sulfate (up to 204 ng (S) m^{-3}) occurs where the DMS emissions are highest over the northern extratropical oceans

(SI Fig. S1) but generally concentrations are in the range 14-78 ng (S) m^{-3} (5^{th} to 95^{th} percentiles of annual mean).

Compared to the total sulfate on an annual basis, iodine aerosol mass is small. Within the marine-boundary layer, the annually averaged iodine aerosol burden is 2.0 Gg (I) which can be compared to 270 Gg (S) for sulfate. Regionally this ratio (I/S as a %) typically lies between 0.3-5.6 % (5^{th} to 95^{th} percentiles) with a maximum of 11% (Figure 2 and zonally in SI Fig. S5). Regions of the tropical marine-boundary layer far from local anthropogenic or volcanic influences and with relatively low DMS emission ratio show the highest significance. This fraction can become as high as 35 % on a monthly basis in these regions. Outside the marine-boundary layer (SI Fig. S3) iodine aerosol contributes negligible mass.

Sulfate from DMS is the primary oceanic secondary aerosol source in the model. Compared to the DMS sulfate source, iodine plays a more significant role than to total sulfate aerosol (Figure 2 and zonally in SI Fig. S5). Again the iodine aerosol burden of 2.0 Gg (I) in the marine-boundary layer can be compared to the 67 Gg (S) due to DMS emissions. Annually this ratio (I/S DMS as a %) lies in the range of 0.75 to 15 % (5^{th} to 95^{th} percentiles) over the tropical oceans with a maximum of 101 %. On a monthly basis, this can increase by in excess of a factor of 4. The iodine to DMS sourced sulfate mass fraction is highest in regions of the tropical marine-boundary layer where the iodine emissions are high and DMS emissions low (Indian ocean and the Pacific coast of Mexico). From an ocean-atmosphere perspective iodine thus appears to play a regionally important role in determining the secondary aerosol load of the marine-boundary layer.

3.4. Pre-industrial concentrations

Understanding the aerosol distribution before human perturbation helps define the direct and indirect effects of aerosol. Our simulation of the pre-industrial is described in Section 2 and previously in *Sherwen et al.* [2016c]. We find lower O_3 concentrations (globally averaged 28 % and 38 % in the marine-boundary layer) in the pre-industrial, consistent with previous studies [*Lamarque et al.*, 2010; *Parrella et al.*, 2012]. This lower O_3 leads to a reduction in the inorganic ocean iodine source of 42 % to 1.25 Tg (I) yr^{-1}. This is higher than the reduction in marine-boundary layer O_3 as the largest reduction in O_3 occurs in the tropics where most of the inorganic iodine emissions occur. Total iodine emissions are thus reduced 33 % to 1.84 Tg (I) yr^{-1}. The iodine processing in the atmosphere changes significantly in the pre-industrial, with the lower NO_X concentrations lengthening the I_y lifetime due to reduced $IONO_2$ hydrolysis. Thus, the iodine aerosol burdens only reduced by 23 % from the present-day. Figure 3 shows the pre-industrial iodine mass concentrations as a fraction of the pre-industrial total sulfate mass concentration. The reduction in the anthropogenic sulfur emissions leads to iodine aerosol being a larger fraction of the total sulfate in the pre-industrial. The global iodine burden of 1.6 Gg (I) in the marine-boundary layer compares to a total sulfate burden of 181 Gg (S). Spatially, iodine aerosol within the atmosphere above the tropical ocean surface can be up to 21 % (0.2-6.8 %, 5^{th} to 95^{th} percentiles) of the total sulfate mass on an annual basis with some locations showing iodine aerosol mass being $\sim$50 % of the sulfate mass in some months. Thus iodine aerosol may have played an important regional role in determining the pre-industrial marine-boundary-layer aerosol load.

4. Implications and conclusions

The size distribution, optical and cloud condensation properties of iodine aerosol are unknown or uncertain, which makes investigating the aerosol radiative impacts of iodine difficult. However studies of aerosol optical depth (AOD) have identified model underprediction compared to satellite observations in marine locations such as the Indian Ocean, Oceania and the Gulf of Guinea where we predict the highest iodine aerosol mass concentrations [*Lapina et al.*, 2011]. An additional source of aerosol in those regions may make a contribution to reconcile observations with models. There is also strong evidence to support the nucleation of new particles from iodine [*O'Dowd et al.*, 2002; *Allan et al.*, 2015; *Roscoe et al.*, 2015; *Sellegri et al.*, 2016]. For regions where nucleation due to sulfur compounds is slow, iodine may be an important source of new particles.

There are still significant uncertainties in the magnitude and impacts of the ocean-atmosphere cycling of iodine. However, it would appear from these calculations that iodine aerosol may play an important regional role in determining the aerosol load of the remote tropical ocean both in the present and in the pre-industrial. Further observations in these regions would help us to constrain the magnitude of this role.

Acknowledgments. This work was funded by NERC quota studentship NE/K500987/1 with support from the NERC BACCHUS and CAST projects NE/L01291X/1, NE/J006165/1.

J. A. Schmidt acknowledges funding through a Carlsberg Foundation post-doctoral fellowship (CF14-0519).

T. Sherwen would like to acknowledge constructive comments and input from GEOS-Chem Support Team.

The model code used here will be made available to the community through the standard GEOS-Chem repository (www.geos-chem.org). Requests for materials should be addressed to Mat Evans (mat.evans@york.ac.uk).

References

Abbatt, J. P. D., A. K. Y. Lee, and J. A. Thornton (2012), Quantifying trace gas uptake to tropospheric aerosol: recent advances and remaining challenges, *Chem. Soc. Rev.*, *41*(19), 6555–6581, doi:10.1039/c2cs35052a.

Alexander, B. (2005), Sulfate formation in sea-salt aerosols: Constraints from oxygen isotopes, *J. Geophys. Res.*, *110*(D10), D10,307, doi:10.1029/2004JD005659.

Alexander, B., D. J. Allman, H. M. Amos, T. D. Fairlie, J. Dachs, D. A. Hegg, and R. S. Sletten (2012), Isotopic constraints on the formation pathways of sulfate aerosol in the marine boundary layer of the subtropical northeast Atlantic Ocean, *J. Geophys. Res.*, *117*(D6), D06,304, doi:10.1029/2011JD016773.

Alicke, B., K. Hebestreit, J. Stutz, and U. Platt (1999), Iodine oxide in the marine boundary layer, *Nature*, *397*(6720), 572–573,

Allan, J. D., P. I. Williams, J. Najera, J. D. Whitehead, M. J. Flynn, J. W. Taylor, D. Liu, E. Darbyshire, L. J. Carpenter, R. Chance, S. J. Andrews, S. C. Hackenberg, and G. McFiggans (2015), Iodine observed in new particle formation events in the Arctic atmosphere during ACCACIA, *Atmospheric Chemistry and Physics*, *15*(10), 5599–5609, doi:10.5194/acp-15-5599-2015.

Ammann, M., R. A. Cox, J. N. Crowley, M. E. Jenkin, A. Mellouki, M. J. Rossi, J. Troe, and T. J. Wallington (2013), Evaluated kinetic and photochemical data for atmospheric chemistry: Volume VI ? heterogeneous reactions with liquid substrates, *Atmos. Chem. Phys.*, *13*, 8045–8228, doi:10.5194/acp-13-8045-2013.

Atkinson, R., D. L. Baulch, R. A. Cox, J. N. Crowley, R. F. Hampson, R. G. Hynes, M. E. Jenkin, M. J. Rossi, J. Troe, and IUPAC Subcommittee (2006), Evaluated kinetic and photochemical data for atmospheric chemistry: Volume II – gas phase reactions of organic species, *Atmos. Chem. Phys.*, *6*(11), 3625–4055, doi:10.5194/acp-6-3625-2006.

Atkinson, R., D. L. Baulch, R. A. Cox, J. N. Crowley, R. F. Hampson, R. G. Hynes, M. E. Jenkin, M. J. Rossi, and J. Troe (2007), Evaluated kinetic and photochemical data for atmospheric chemistry: Volume III - gas phase reactions of inorganic halogens, *Atmos. Chem. Phys.*, *7*, 981–1191.

Atkinson, R., D. L. Baulch, R. A. Cox, J. N. Crowley, R. F. Hampson, R. G. Hynes, M. E. Jenkin, M. J. Rossi, J. Troe, and T. J. Wallington (2008), Evaluated kinetic and photochemical data for atmospheric chemistry: Volume IV - gas phase reactions of organic halogen species, *J. Phys. Chem. Ref. Data*, *8*(15), 4141–4496.

Baker, A. R., Tunnicliffe C., and Jickells T. D. (2001), Iodine speciation and deposition fluxes from the marine atmosphere, *Journal of Geophysical Research*, *106*(D22), 28,743–28,749.

Baker, A. R. (2004), Inorganic iodine speciation in tropical Atlantic aerosol, *Geophysical Research Letters*, *31*(23), L23S02, doi:10.1029/2004GL020144.

Baker, A. R. (2005), Marine aerosol iodine chemistry: The importance of soluble organic iodine, *Environ. Chem.*, *2*(4), 295–298, doi:10.1071/en05070.

Bell, N., L. Hsu, D. J. Jacob, M. G. Schultz, D. R. Blake, J. H. Butler, D. B. King, J. M. Lobert, and E. Maier-Reimer (2002), Methyl iodide: Atmospheric budget and use as a tracer of marine convection in global models, *J. Geophys. Res-Atmos.*, *107*(D17), ACH 8–1–ACH 8–12, doi:10.1029/2001jd001151.

Braban, C. F., J. W. Adams, D. Rodriguez, R. A. Cox, J. N. Crowley, and G. Schuster (2007), Heterogeneous reactions of HOI, ICl and IBr on sea salt and sea salt proxies, *Phys. Chem. Chem. Phys.*, *9*(24), 3136–3148, doi:10.1039/b700829e.

Carpenter, L. J., S. M. MacDonald, M. D. Shaw, R. Kumar, R. W. Saunders, R. Parthipan, J. Wilson, and J. M. C. Plane (2013), Atmospheric iodine levels influenced by sea surface emissions of inorganic iodine, *Nature Geosci.*, *6*(2), 108–111, doi:10.1038/ngeo1687.

Carslaw, K. S., L. A. Lee, C. L. Reddington, K. J. Pringle, A. Rap, P. M. Forster, G. W. Mann, D. V. Spracklen, M. T. Woodhouse, L. A. Regayre, and J. R. Pierce (2013), Large contribution of natural aerosols to uncertainty in indirect forcing, *Nature*, *503*(7474), 67–71.

Chance, R., T. D. Jickells, and A. R. Baker (2015), Atmospheric trace metal concentrations, solubility and deposition fluxes in remote marine air over the south-east Atlantic, *Marine Chemistry*, *177, Part*, 45–56, doi: http://dx.doi.org/10.1016/j.marchem.2015.06.028.

Eastham, S. D., D. K. Weisenstein, and S. R. H. Barrett (2014), Development and evaluation of the unified tropospheric?stratospheric chemistry extension (UCX) for the global chemistry-transport model GEOS-Chem, *Atmos. Environ.*, *89*, 52–63, doi:http://dx.doi.org/10.1016/j.atmosenv.2014.02.001.

Fitzgerald, J. W. (1991), Marine aerosols: A review, *Atmospheric Environment. Part A. General Topics*, *25*(3-4), 533–545, doi:10.1016/0960-1686(91)90050-H.

Gilfedder, B. S., R. Chance, U. Dettmann, S. C. Lai, and A. R. Baker (2010), Determination of total and non-water soluble iodine in atmospheric aerosols by thermal extraction and spectrometric detection (TESI), *Analytical and Bioanalytical Chemistry*, *398*(1), 519–526, doi:10.1007/s00216-010-3923-1.

Hausmann, M., and U. Platt (1994), Spectroscopic measurement of bromine oxide and ozone in the high Arctic during Polar Sunrise Experiment 1992, *Journal of Geophysical Research*, *99*(D12), 25,399, doi:10.1029/94JD01314.

Jaeglé, L., P. K. Quinn, T. S. Bates, B. Alexander, and J. T. Lin (2011), Global distribution of sea salt aerosols: new constraints from in situ and remote sensing observations, *Atmos. Chem. Phys.*, *11*(7), 3137–3157, doi:10.5194/acp-11-3137-2011.

Jones, C. E., K. E. Hornsby, R. Sommariva, R. M. Dunk, R. Von Glasow, G. McFiggans, and L. J. Carpenter (2010), Quantifying the contribution of marine organic gases to atmospheric iodine, *Geophys. Res. Lett.*, *37*(18), L18,804, doi:10.1029/2010gl043990.

Kettle, A. J., M. O. Andreae, D. Amouroux, T. W. Andreae, T. S. Bates, H. Berresheim, H. Bingemer, R. Boniforti, M. A. J. Curran, G. R. DiTullio, G. Helas, G. B. Jones, M. D. Keller, R. P. Kiene, C. Leck, M. Levasseur, G. Malin, M. Maspero, P. Matrai, A. R.

McTaggart, N. Mihalopoulos, B. C. Nguyen, A. Novo, J. P. Putaud, S. Rapsomanikis, G. Roberts, G. Schebeske, S. Sharma, R. Simó, R. Staubes, S. Turner, and G. Uher (1999), A global database of sea surface dimethylsulfide (DMS) measurements and a procedure to predict sea surface DMS as a function of latitude, longitude, and month, *Global Biogeochemical Cycles*, *13*(2), 399–444, doi:10.1029/1999GB900004.

Lai, S. C., T. Hoffmann, and Z. Q. Xie (2008), Iodine speciation in marine aerosols along a 30,000 km round-trip cruise path from Shanghai, China to Prydz Bay, Antarctica, *Geophysical Research Letters*, *35*(21), L21,803, doi:10.1029/2008GL035492.

Lamarque, J.-F., T. C. Bond, V. Eyring, C. Granier, A. Heil, Z. Klimont, D. Lee, C. Liousse, A. Mieville, B. Owen, M. G. Schultz, D. Shindell, S. J. Smith, E. Stehfest, J. Van Aardenne, O. R. Cooper, M. Kainuma, N. Mahowald, J. R. McConnell, V. Naik, K. Riahi, and D. P. van Vuuren (2010), Historical (1850?2000) gridded anthropogenic and biomass burning emissions of reactive gases and aerosols: methodology and application, *Atmos. Chem. Phys.*, *10*(15), 7017–7039, doi:10.5194/acp-10-7017-2010.

Lapina, K., C. L. Heald, D. V. Spracklen, S. R. Arnold, J. D. Allan, H. Coe, G. McFiggans, S. R. Zorn, F. Drewnick, T. S. Bates, L. N. Hawkins, L. M. Russell, A. Smirnov, C. D. O'Dowd, and A. J. Hind (2011), Investigating organic aerosol loading in the remote marine environment, *Atmospheric Chemistry and Physics*, *11*(17), 8847–8860, doi:10.5194/acp-11-8847-2011.

Liss, P., and L. Merlivat (1986), Air-Sea Gas Exchange Rates: Introduction and Synthesis, in *The Role of Air-Sea Exchange in Geochemical Cycling SE - 5*, *NATO ASI Series*, vol. 185, edited by P. Buat-Ménard, pp. 113–127, Springer Netherlands,

Lovelock, J. E., R. J. MAGGS, and R. A. RASMUSSEN (1972), Atmospheric Dimethyl Sulphide and the Natural Sulphur Cycle, *Nature*, *237*(5356), 452–453.

MacDonald, S. M., J. C. Gómez Martín, R. Chance, S. Warriner, A. Saiz-Lopez, L. J. Carpenter, and J. M. C. Plane (2014), A laboratory characterisation of inorganic iodine emissions from the sea surface: dependence on oceanic variables and parameterisation for global modelling, *Atmos. Chem. Phys.*, *14*(11), 5841–5852, doi:10.5194/acp-14-5841-2014.

McElroy, C. T., C. A. McLinden, and J. C. McConnell (1999), Evidence for bromine monoxide in the free troposphere during the Arctic polar sunrise, *Nature*, *397*(6717), 338–341.

O'Dowd, C. D., J. L. Jimenez, R. Bahreini, R. C. Flagan, J. H. Seinfeld, K. Hameri, L. Pirjola, M. Kulmala, S. G. Jennings, and T. Hoffmann (2002), Marine aerosol formation from biogenic iodine emissions, *Nature*, *417*(6889), 632–636.

Ordóñez, C., J. F. Lamarque, S. Tilmes, D. E. Kinnison, E. L. Atlas, D. R. Blake, G. S. Santos, G. Brasseur, and A. Saiz-Lopez (2012), Bromine and iodine chemistry in a global chemistry-climate model: description and evaluation of very short-lived oceanic sources, *Atmos. Chem. Phys.*, *12*(3), 1423–1447, doi:10.5194/acp-12-1423-2012.

Park, R. J., D. J. Jacob, B. D. Field, R. M. Yantosca, and M. Chin (2004), Natural and transboundary pollution influences on sulfate-nitrate-ammonium aerosols in the United States: Implications for policy, *J Geophys. Res-Atmos.*, *109*(D15), n/a—-n/a, doi:10.1029/2003JD004473.

Parrella, J. P., D. J. Jacob, Q. Liang, Y. Zhang, L. J. Mickley, B. Miller, M. J. Evans, X. Yang, J. A. Pyle, N. Theys, and M. Van Roozendael (2012), Tropospheric bromine chemistry: implications for present and pre-industrial ozone and mercury, *Atmos. Chem. Phys.*, *12*(15), 6723–6740, doi:10.5194/acp-12-6723-2012.

Pechtl, S., G. Schmitz, and R. von Glasow (2007), Modelling iodide-iodate speciation in atmospheric aerosol: Contributions of inorganic and organic iodine chemistry, *Atmos. Chem. Phys.*, *7*, 1381–1393.

Powell, C. F., A. R. Baker, T. D. Jickells, H. W. Bange, R. J. Chance, and C. Yodle (2015), Estimation of the Atmospheric Flux of Nutrients and Trace Metals to the Eastern Tropical North Atlantic Ocean, *J. Atmos. Sci.*, *72*(10), 4029–4045, doi:10.1175/JAS-D-15-0011.1.

Rancher, J., and M. A. Kritz (1980), Diurnal fluctuations of Br and I in the tropical marine atmosphere, *Journal of Geophysical Research: Oceans*, *85*(C10), 5581–5587, doi:10.1029/JC085iC10p05581.

Rap, A., C. E. Scott, D. V. Spracklen, N. Bellouin, P. M. Forster, K. S. Carslaw, A. Schmidt, and G. Mann (2013), Natural aerosol direct and indirect radiative effects, *Geophys. Res. Lett.*, *40*(12), 3297–3301, doi:10.1002/grl.50441.

Roscoe, H. K., A. E. Jones, N. Brough, R. Weller, A. Saiz-Lopez, A. S. Mahajan, A. Schoenhardt, J. P. Burrows, and Z. L. Fleming (2015), Particles and iodine compounds in coastal Antarctica, *J Geophys. Res-Atmos.*, *120*(14), 7144–7156, doi:10.1002/2015JD023301.

Saiz-Lopez, A., and R. von Glasow (2012), Reactive halogen chemistry in the troposphere, *Chem. Soc. Rev.*, *41*(19), 6448–6472, doi:10.1039/c2cs35208g.

Saiz-Lopez, A., A. S. Mahajan, R. A. Salmon, S. J. B. Bauguitte, A. E. Jones, H. K. Roscoe, and J. M. C. Plane (2007), Boundary layer halogens in coastal Antarctica, *Science*, *317*(5836), 348–351, doi:10.1126/science.1141408.

Saiz-Lopez, A., J. M. C. Plane, A. R. Baker, L. J. Carpenter, R. von Glasow, J. C. G. Martin, G. McFiggans, and R. W. Saunders (2012a), Atmospheric Chemistry of Iodine, *Chem. Rev.*, *112*(3), 1773–1804, doi:10.1021/cr200029u.

Saiz-Lopez, A., J. F. Lamarque, D. E. Kinnison, S. Tilmes, C. Ordonez, J. J. Orlando, A. J. Conley, J. M. C. Plane, A. S. Mahajan, G. S. Santos, E. L. Atlas, D. R. Blake, S. P. Sander, S. Schauffler, A. M. Thompson, and G. Brasseur (2012b), Estimating the climate significance of halogen-driven ozone loss in the tropical marine troposphere, *Atmos. Chem. Phys.*, *12*(9), 3939–3949, doi:10.5194/acp-12-3939-2012.

Saiz-Lopez, A., R. P. Fernandez, C. Ordóñez, D. E. Kinnison, J. C. Gómez Martín, J.-F. Lamarque, and S. Tilmes (2014), Iodine chemistry in the troposphere and its effect on ozone, *Atmos. Chem. Phys..*, *14*(14), 19,985–20,044, doi:10.5194/acpd-14-19985-2014.

Sander, S. P., R. R. Friedl, J. P. D. Abbatt, J. R. Barker, J. B. Burkholder, D. M. Golden, C. E. Kolb, M. J. Kurylo, G. K. Moortgat, P. H. Wine, R. E. Huie, and V. L. Orkin (2011), Chemical kinetics and photochemical data for use in atmospheric studies, Evaluation Number 17, *Tech. rep.*, NASA Jet Propulsion Laboratory.

Schmidt, J. A., D. J. Jacob, H. M. Horowitz, L. Hu, T. Sherwen, M. J. Evans, Q. Liang, R. M. Suleiman, D. E. Oram, M. L. Breton, C. J. Percival, S. Wang, B. Dix, and

R. Volkamer (2016), Modeling the observed tropospheric BrO background: Importance of multiphase chemistry and implications for ozone, OH, and mercury, *J Geophys. Res-Atmos.*

Sellegri, K., J. Pey, C. Rose, A. Culot, H. L. DeWitt, S. Mas, A. N. Schwier, B. Temime-Roussel, B. Charriere, A. Saiz-Lopez, A. S. Mahajan, D. Parin, A. Kukui, R. Sempere, B. D'Anna, and N. Marchand (2016), Evidence of atmospheric nanoparticle formation from emissions of marine microorganisms, *Geophysical Research Letters*, pp. n/a—-n/a, doi:10.1002/2016GL069389.

Sherwen, T., M. J. Evans, L. J. Carpenter, S. J. Andrews, R. T. Lidster, B. Dix, T. K. Koenig, R. Sinreich, I. Ortega, R. Volkamer, A. Saiz-Lopez, C. Prados-Roman, A. S. Mahajan, and C. Ordóñez (2016a), Iodine's impact on tropospheric oxidants: a global model study in GEOS-Chem, *Atmos. Chem. Phys.*, *16*(2), 1161–1186, doi:10.5194/acp-16-1161-2016.

Sherwen, T., J. A. Schmidt, M. J. Evans, L. J. Carpenter, K. Großmann4, S. D. Eastham, D. J. J., B. Dix, T. K. Koenig, R. Sinreich, I. Ortega, R. Volkamer, A. Saiz-Lopez, C. Prados-Roman, A. S. Mahajan, and C. Ordóñez (2016b), Global impacts of tropospheric halogens (Cl, Br, I) on oxidants and composition in GEOS-Chem, *Atmos. Chem. Phys. Discuss.*

Sherwen, T., M. J. Evans, L. J. Carpenter, J. A. Schmidt, and L. J. Mickely (2016c), Halogen chemistry reduces tropospheric O3 radiative forcing, *Atmospheric Chemistry and Physics Discussions*, pp. 1–18, doi:10.5194/acp-2016-688.

Simpson, W. R., S. S. Brown, A. Saiz-Lopez, J. A. Thornton, and R. von Glasow (2015), Tropospheric Halogen Chemistry: Sources, Cycling, and Impacts, *Chemical Reviews*, *115*(10), 4035–4062, doi:10.1021/cr5006638.

Sommariva, R., W. J. Bloss, and R. von Glasow (2012), Uncertainties in gas-phase atmospheric iodine chemistry, *Atmos. Environ.*, *57*, 219–232, doi: 10.1016/j.atmosenv.2012.04.032.

Stocker, T., D. Qin, G.-K. Plattner, M. Tignor, S. Allen, J. Boschung, A. Nauels, Y. Xia, V. Bex, and P. M. (eds.) (2000), IPCC, 2013: Climate Change 2013: The Physical Science Basis. Contribution of Working Group I to the Fifth Assessment Report of the Intergovernmental Panel on Climate Change, *Tech. rep.*, Cambridge University Press, Cambridge, United Kingdom and New York, NY, USA, doi: 10.1017/CBO9781107415324.

Tuckermann, M., R. Ackermann, C. Gölz, H. Lorenzen-Schmidt, T. Senne, J. Stutz, B. Trost, W. Unold, and U. Platt (1997), {DOAS}-observation of halogen radical- catalysed {A}rctic boundary layer ozone destruction during the {ARCTOC} campaign 1995 and 1996 in {Ny-Alesund}, {S}pitsbergen, *Tellus*, *49b*(5), 533–555, doi:10.1034/j.1600-0889.49.issue5.9.x.

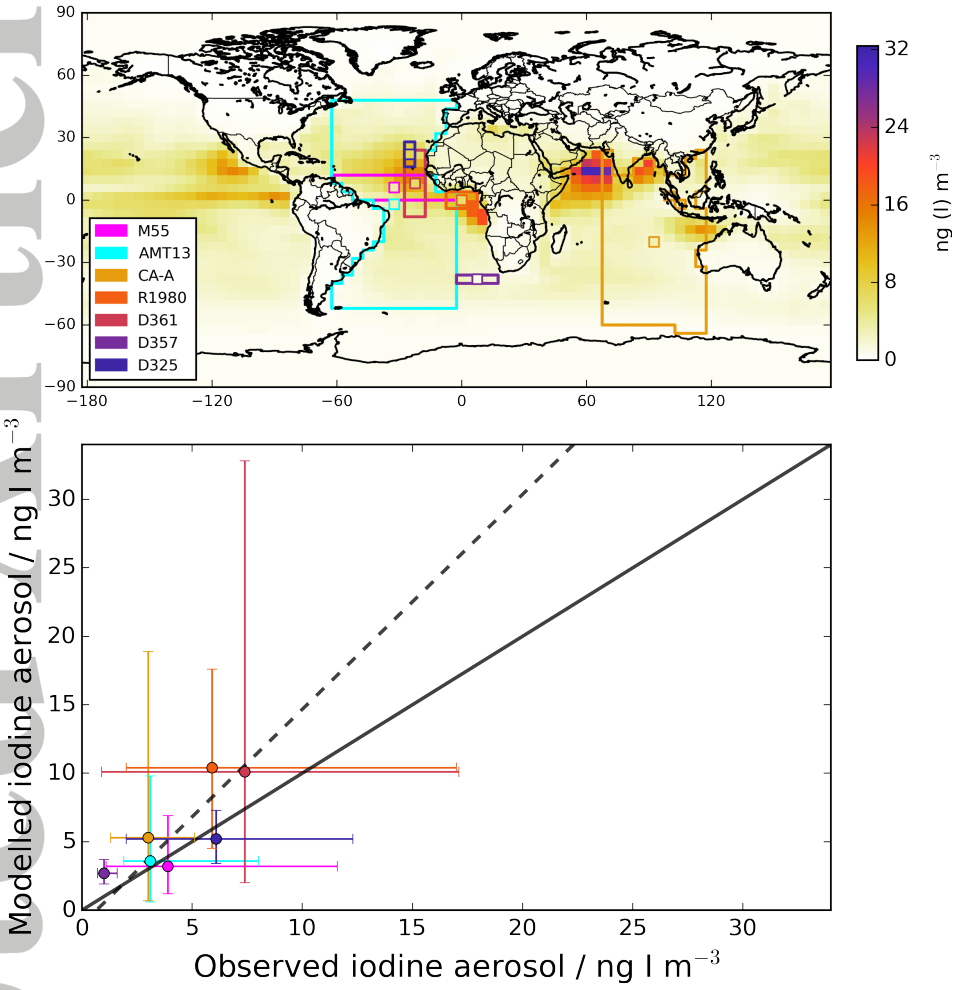

Figure 1. Simulated and observed surface iodine aerosol. Background of the upper plot is the modelled annual-mean surface aerosol mass concentrations (ng (I) m^{-3}). Observations (small coloured squares) indicate the average value reported by individual studies [*Baker*, 2004, 2005; *Gilfedder et al.*, 2010; *Lai et al.*, 2008; *Rancher and Kritz*, 1980] and datasets "D325", "D357", and "D361" are described in the supplementary material. The small coloured square is located at the centre of the domain (large coloured region). Lower plot shows the observed mean values with the error bar representing the reported maximum and minimum. Each modelled point represents the mean value in the region shown in the top plot with the error bar representing the 5 and 95^{th} percentile of the distribution in that region. The colors of the points are the same as the areas on the map. The continuous black line is the 1:1 line, and the dashed line is the orthogonal linear regression best fit.

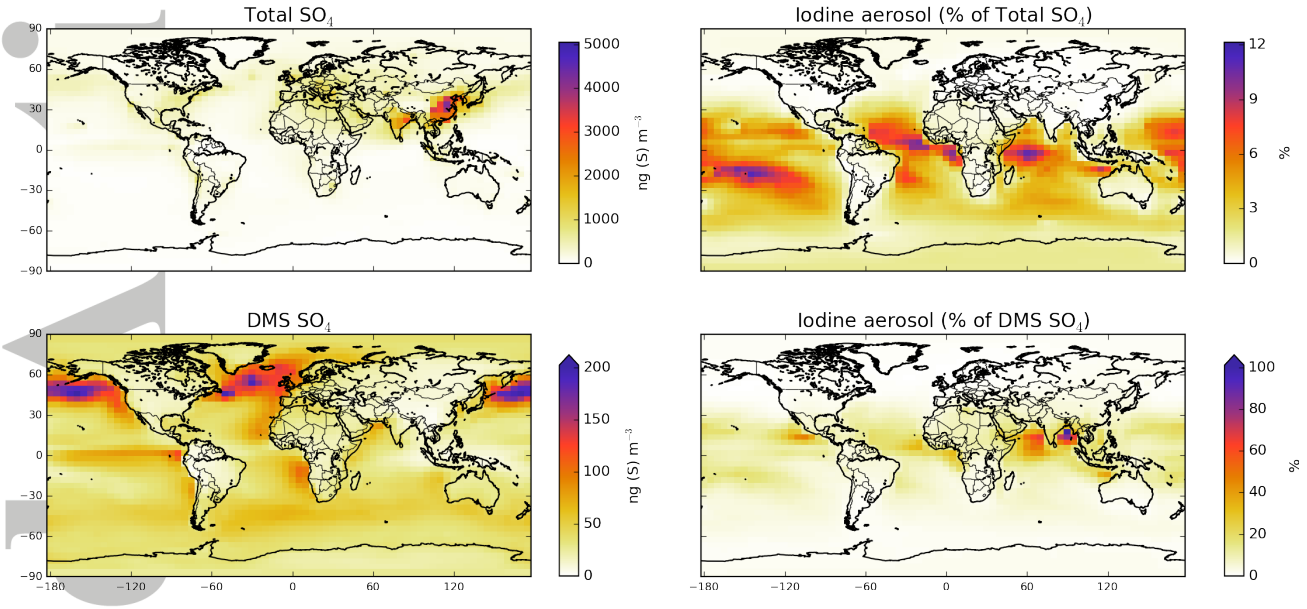

Figure 2. Annual average present-day modelled surface mass concentrations of total (upper left) and DMS (lower left) sourced SO_4^{2-} aerosol in ng S m^{-3} (left). Iodine mass fraction (ng (I) m^{-3}) as % of sulfate species is shown on the (right).

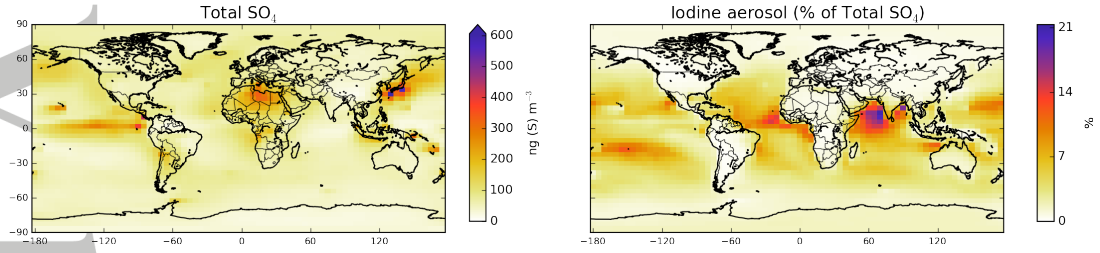

Figure 3. Annual average pre-industrial modelled surface mass concentrations of total sulfate (ng S m^{-3}, left) and the mass of iodine aerosol (ng (I) m^{-3}) as a fraction of this (right).